1-1-2012

Microscopic model of a phononic refrigerator

Liliana Arrachea

Eduardo R. Mucciolo
University of Central Florida

Claudio Chamon

Rodrigo B. Capaz

Microscopic model of a phononic refrigerator

Liliana Arrachea,[1] Eduardo R. Mucciolo,[2] Claudio Chamon,[3] and Rodrigo B. Capaz[4]

[1]*Departamento de Física, FCEyN and IFIBA, Universidad de Buenos Aires, Pabellón 1, Ciudad Universitaria, 1428 Buenos Aires, Argentina*

[2]*Department of Physics, University of Central Florida, Orlando, Florida 32816, USA*

[3]*Department of Physics, Boston University, Boston, Massachusetts 02215, USA*

[4]*Instituto de Física, Universidade Federal do Rio de Janeiro, Caixa Postal 68528, Rio de Janeiro 21941-972, Rio de Janeiro, Brazil*

(Received 12 March 2012; published 17 September 2012)

We analyze a simple microscopic model to pump heat from a cold to a hot reservoir in a nanomechanical system. The model consists of a one-dimensional chain of masses and springs coupled to a back gate through which a time-dependent perturbation is applied. The action of the gate creates a moving phononic barrier by locally pinning a mass. We solve the problem numerically using a nonequilibrium Green's function technique. For low driving frequencies and for sharp traveling barriers, we show that this microscopic model realizes a phonon refrigerator.

DOI: 10.1103/PhysRevB.86.125424 PACS number(s): 63.22.Gh, 65.80.−g

I. INTRODUCTION

In atomic gases, techniques such as evaporative cooling can bring temperatures down to the submicrokelvin scale, allowing for the observation of quantum phenomena such as Bose-Einstein condensation. Progress in refrigerating condensed-matter systems has been less spectacular but steady; a recent example is the use of active feedback for cooling nanomechanical cantilevered beams.[1] Other experimental examples, most of them in electronic devices, have been reviewed in Ref. 2. On the theoretical side, mechanisms for quantum refrigeration by means of electronic pumping with ac fields operating at low[3] and high[4] frequencies have been proposed recently. There are also several proposals for cooling nanomechanical systems by absorbing phonons with electrons.[5]

The challenge of quantum refrigeration is to keep the heat extracted from the cold sample higher than the energy dissipated into it by operating the cooling machine. In electronic ac pumping, this condition can be achieved within the so-called "adiabatic" quantum-pumping regime. For instance, in mesoscopic structures, this regime is attained by modulating electronic potentials with two low-frequency fields with a relative phase.[3] More precisely, assuming that the electrons propagate coherently through such a device, it can be shown that heat is pumped at a rate proportional to $k_B T \Omega_0$, while the rate at which energy is dissipated scales as $\hbar \Omega_0^2$, where T is the temperature of the cold reservoir and Ω_0 is the frequency of the ac field. As in the cases of charge[6,7] and spin[8] pumping, coherence is expected to be an important ingredient for this type of heat pumping. These mechanisms act on the electronic degrees of freedom, and therefore they are ineffective in cooling insulators. Cooling procedures based on phonon manipulation, however, apply equally well to metals and insulators. Phononic refrigeration is the topic of this paper.

The minimal microscopic model for acoustic phonons consists of masses coupled by springs. Heat transport and thermalization in chains of coupled oscillators have a rather long history in statistical physics since the pioneer work by Fermi *et al.*[9] Several studies of different classical and quantum models have analyzed the local temperature profile of chains of coupled oscillators in contact with two reservoirs at different temperatures.[10] The striking feature found in these studies was the violation of the Fourier law, according to which the local temperature is expected to drop linearly along the chain. This behavior is the phononic counterpart of the abrupt drop of the local voltage at the connections between a finite-size electronic system to two reservoirs at different chemical potentials, which has been characterized by the concept of "contact resistance."[11] More recently, heat pumping has been analyzed through a two-level system driven by an ac field coupled to phononic baths at different temperatures,[12] between semi-infinite harmonic chains with a time-dependent coupling,[13] and in anharmonic molecular junctions in contact with phononic baths.[14]

In a recent work,[15] we have shown that when a barrier (or perturbation) moves along a cavity (which we refer to as pipe) connecting two gases of acoustic phonons, a sizable amount of heat can be transferred from the colder to the hotter gas. Assuming that the barrier is perfectly reflective and its motion is slow enough to allow for a fast thermalization of the phonon gas, we can imagine a cycle where (i) a barrier is inserted at the end of the pipe close to the cold reservoir; (ii) the barrier is then adiabatically translated through the pipe until it reaches the end in contact to the hot reservoir; (iii) a second barrier is then inserted again near the cold reservoir; and (iv) the first barrier is finally removed. The process can then be repeated as a cycle. The result is a refrigerator which does not rely on quantum coherence.

The phonon pump proposed in Ref. 15 used a thermodynamical formulation for the phonon gas. Here we present instead a microscopic model of acoustic phonons that implements this cooling scheme. The lattice model we consider consists of a series of atoms or molecules with identical masses coupled by springs. The moving barrier in this microscopic model is realized by modulating in time and space a local pinning potential, which restricts the longitudinal motion of the particles. The setup is shown schematically in Fig. 1.

The paper is organized as follows. In Sec. II we present the microscopic model. In Sec. III A, we show the result of numerical computations of the heat currents and use it to evaluate the lowest temperature the phonon pump can cool down. This result is then compared to the prediction made

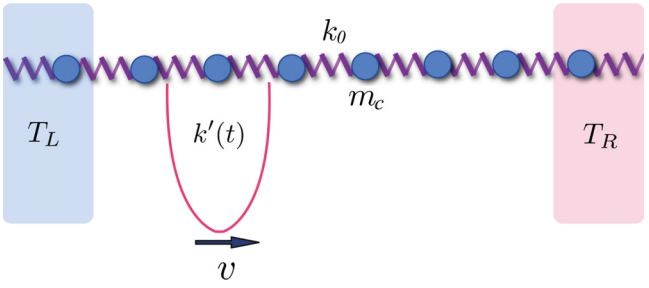

FIG. 1. (Color online) The one-dimensional microscopic model for acoustic phonons consists of a chain of particles (atoms of molecules) with equal mass m_c coupled by springs with elastic constants k_0. The semi-infinite left portion of the chain is kept at a temperature T_L which is lower than the temperature T_R of the semi-infinite right portion. A traveling harmonic potential is applied locally to the central portion of the chain. This potential restricts the longitudinal motion of the particles—see the last term on the right-hand side of Eq. (2). To perform a cooling cycle, the local potential is turned on and moved from near the cold to the hot reservoir at a constant speed v. When it reaches the hot reservoir, the potential is turned off and moved back to near the cold reservoir.

in Ref. 15 based on a continuum model. In Sec. IV we provide a detailed description of the nonequilibrium Green's function methodology used to carry out the computations. Our conclusions are presented in Sec. V. Some technical details are presented in the appendixes.

II. MICROSCOPIC MODEL

We consider the one-dimensional (1d) system sketched in Fig. 1, with a central finite chain of N atoms or molecules (which we refer to as "masses" hereafter) with identical masses m_c coupled by springs of constant k_c. This system is connected at its left (right) end to a semi-infinite chain L (R) of masses m_L (m_R) coupled by springs of constant k_L (k_R). These left and right chains play the role of reservoirs, which we assume are kept at temperatures T_L and T_R, respectively. We consider only longitudinal vibrational modes. The ensuing Hamiltonian reads

$$H = H_L + H_R + H_c(t) + H_{\rm cont}. \tag{1}$$

The first two terms $H_{L,R}$ represent the reservoirs; the third $H_c(t)$ describes the central chain, which serves as the pump and has an explicit time dependence; the last term provides the contact between the central chain c and the L,R reservoirs.

The masses in the central chain are coupled to their neighbors via time-independent springs. An external potential is applied to the central part of the chain in order to restrict (i.e., pin) the longitudinal motion of the masses. We use a local harmonic approximation for this pinning potential. (We defer to Sec. V a discussion about the possible experimental realizations.) The ensuing Hamiltonian reads

$$H_c(t) = \sum_{l=1}^{N} \frac{p_{c,l}^2}{2m_c} + \sum_{l=1}^{N-1} \frac{k_0}{2}(x_{c,l} - x_{c,l+1})^2 + \sum_{l=1}^{N} \frac{k_l'(t)}{2}\, x_{c,l}^2. \tag{2}$$

To illustrate the heat pumping mechanism, we break down the spring constant of the local pinning potential into a train of pulses with a Gaussian shape,

$$k_l'(t) = \sum_{n=-\infty}^{+\infty} k_l^{(n)}(t), \tag{3}$$

with $k_l^{(n)}(t) = k_1\, e^{-[al - v(t-n\tau)]^2/\sigma^2}$, $n\tau \leqslant t \leqslant (n+1)\tau$, where a is the lattice constant. The barrier speed is v, its width is σ, and the time it takes to traverse the central chain is $\tau = aN/v$. It is useful to define two characteristic frequencies in the problem: the frequency $\omega_c = \sqrt{k_0/m_c}$ and the pumping frequency $\Omega_0 = 2\pi/\tau$. (We work on units such that $\hbar = k_B = 1$.)

The contact between the central system and the reservoirs is described by the Hamiltonian

$$H_{\rm cont} = \frac{k_L}{2}(x_{L,1} - x_{c,1})^2 + \frac{k_R}{2}(x_{R,1} - x_{c,N})^2. \tag{4}$$

Notice that the central region couples to the left reservoir at the site $l = 1$ and to the right one at $l = N$ (for later use, it is convenient to define $l_L \equiv 1$, $l_R \equiv N$).

The reservoir Hamiltonians are given by

$$H_\alpha = \sum_{j=1}^{N_\alpha} \left[\frac{p_{\alpha,j}^2}{2m_\alpha} + \frac{k_\alpha}{2}(x_{\alpha,j} - x_{\alpha,j+1})^2 \right], \tag{5}$$

with $\alpha = L,R$, in the limit of $N_\alpha \to \infty$ (which we take in due time). The lattice sites are labeled from right to left for the L reservoir and from left to right for the R reservoir. It is convenient to express the degrees of freedom of the L and R reservoirs in terms of normal modes. For open boundary conditions, this corresponds to performing the following transformation:

$$x_{\alpha,l} = \sqrt{\frac{2}{N_\alpha + 1}} \sum_{n=0}^{N_\alpha} \sin\left(q_n^\alpha l\right)\, x_{\alpha,n} \tag{6}$$

and

$$p_{\alpha,l} = \sqrt{\frac{2}{N_\alpha + 1}} \sum_{n=0}^{N_\alpha} \sin\left(q_n^\alpha l\right)\, p_{\alpha,n}, \tag{7}$$

where

$$q_n^\alpha = \frac{n\pi}{N_\alpha + 1}, \quad n = 0, \ldots, N_\alpha. \tag{8}$$

The corresponding Hamiltonians transform into

$$H_\alpha = \sum_n \left\{ \frac{p_{\alpha,n}^2}{2m_\alpha} + \frac{k_\alpha}{2}\left[1 - \cos\left(q_n^\alpha\right)\right] x_{\alpha,n}^2 \right\}. \tag{9}$$

A. Energy balance

Following a procedure similar to that used in Ref. 3, we consider the variation in time of the energy stored in one of the reservoirs. We find

$$\frac{dE_\alpha(t)}{dt} = J_\alpha^Q(t) + P_{l_\alpha}(t), \tag{10}$$

where the first term is the heat current flowing from the connecting site l_α of the central chain into the $\alpha = L,R$

reservoir, which reads

$$J_{\alpha}^{Q}(t) = \sum_{n} k_{n,\alpha} \langle x_{\alpha,n}\, \dot{x}_{l_\alpha} \rangle, \tag{11}$$

with $k_{n,\alpha} = k_\alpha \sqrt{\frac{2}{N_\alpha+1}} \sin(q_n^\alpha)$, while

$$P_{l_\alpha}(t) = \frac{\partial}{\partial t} k'_{l_\alpha}(t) \langle x_{l_\alpha}^2 \rangle \tag{12}$$

is the power due to the time-dependent forces acting at the connecting site l_α.

Conservation of energy implies that the *total* power invested by the external fields is dissipated into the reservoirs at a rate

$$\overline{J}_L^Q + \overline{J}_R^Q = \sum_{l=1}^{N} \overline{P}_l, \tag{13}$$

where

$$\overline{P}_l = \frac{1}{\tau} \int_0^\tau dt\, P_l(t) \tag{14}$$

is the power developed by the external fields at the site l averaged over one period, while

$$\overline{J}_\alpha^Q = \frac{1}{\tau} \int_0^\tau dt\, J_\alpha^Q(t) \tag{15}$$

is the dc component of the heat current at the reservoir α.

Notice that a net amount of work has to be invested in order to pump heat from one reservoir to the other. Carrying out an analysis similar to that developed in Ref. 3 leads us to the conclusion that the rate at which the total work done by the external fields is dissipated as heat flowing into the reservoirs is proportional to Ω_0^2.

In the case of heat transport induced by a temperature gradient between the reservoirs, and in the absence of time-dependent perturbations, the heat current (15) can be expressed in general as

$$J_\alpha^{(0)} = \sum_{\beta=L,R} \int_{-\infty}^{+\infty} \frac{d\omega}{2\pi} \omega [n_\beta(\omega) - n_\alpha(\omega)] \mathcal{T}(\omega), \tag{16}$$

where $\mathcal{T}(\omega)$ is the thermal transmission function of the structure, while $n_\alpha(\omega)$ is the Bose-Einstein distribution function, which depends of the temperature of the reservoir α.

We evaluate these physical quantities by employing the nonequilibrium Green's function formalism. Before describing the technical details of the calculations, we first present the results that demonstrate the refrigeration capabilities of the phonon pump.

III. PHONONIC REFRIGERATION

A. Mechanism and minimum cooling temperature

We now show results for the heat currents corresponding to a perturbation of the form of a train of traveling Gaussian pulses described by the modulation shown in Eq. (3). The main goal here is to compare the results obtained for our microscopic phononic system to the predictions put forward in Ref. 15, which were derived for a continuum model system with a strong, δ-like traveling perturbation. As mentioned in Sec. II A and Ref. 3, the rate at which heat is produced is proportional to Ω_0^2. Therefore, we consider a low driving frequency $\Omega_0 = 2\pi/\tau$ in order to ensure a low rate of heat dissipation into the reservoirs and to achieve a regime where heat can be effectively transported from the cold to the hot reservoir. The speed of the barrier is tuned to $v = aN/\tau$, such that a new pulse appears on the left end of the central region every time a pulse moves through the right end.

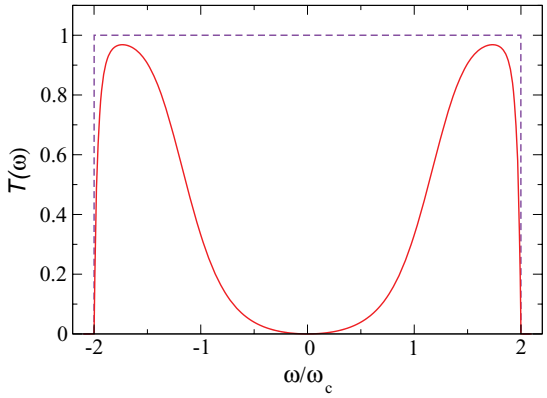

FIG. 2. (Color online) The transmission function $\mathcal{T}(\omega)$ defined in Eq. (42) for a central system of $N = 40$ atoms without any barrier (dashed lines) and with a Gaussian barrier with height $k_1 = 1.5k_0$ and $\sigma = a$ (solid lines) centered at $l = 20$. The frequency is shown in units of the chain's characteristic frequency $\omega_c = \sqrt{k_0/m_c}$.

Before showing the results for the dc heat current, it is interesting to analyze the effect of a stationary ($v = 0$) pinning potential on the behavior of the heat transmission function $\mathcal{T}(\omega)$ [see Eq. (42)]. This is illustrated in Fig. 2, where $\mathcal{T}(\omega)$ is shown for both the unperturbed chain ($k_1 = 0$) and the case with a narrow, time-independent Gaussian spatial modulation near the center of the chain. It is clear from Fig. 2 that the effect of the pinning potential is to decrease the transmission probability in the low-energy sector of the phonon spectrum. Such an effect is an indication that the pinning potential, when stationary at a certain site, acts like a barrier, blocking heat transport from the hot to the cold reservoir.

In Ref. 15 we have shown that besides blocking the usual heat flowing in the direction of the heat gradient, a moving barrier in a phonon gas also enables refrigeration under certain conditions. Figure 3 demonstrates that this is also the case of the microscopic model considered in the present work. We consider a finite-size central chain with $N = 80$ atoms and a low pumping frequency $\Omega_0 = 1 \times 10^{-5}\, \omega_c$. We fix the temperature of the hot reservoir at $T_R = 0.04\, \omega_c$ and analyze the behavior of the heat current at the contacts between the central system and each of the reservoirs. In Fig. 3, we can see that for large temperature differences $\Delta T = T_R - T_L$ the dc heat current at the cold reservoir is positive, indicating that the flow enters this reservoir, while it is negative at the hot one (the flow exits that reservoir). In this situation, the direction of the heat current is ruled by the heat gradient (hot to cold). As ΔT decreases, there is a range of temperatures of the cold reservoir, $T^* \leqslant T_L \leqslant T_{\min}$, where the two currents flowing into the reservoirs become positive. When the temperature of the cold reservoir overcomes $T_{\min}$, $\overline{J}_L^Q < 0$ and $\overline{J}_R^Q > 0$. In this regime, there is a net heat flow from the cold to the hot reservoir, which means that the system operates like a

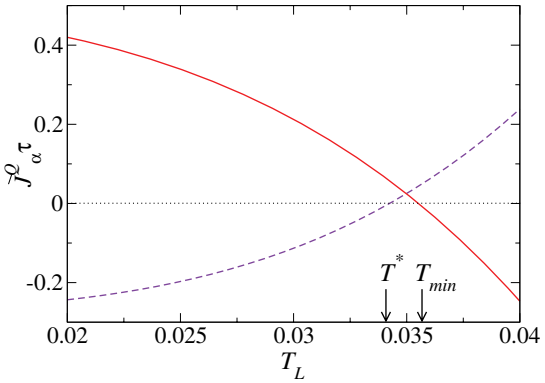

FIG. 3. (Color online) The average energy flowing through the contacts in a cycle, $\bar{J}^Q_\alpha \tau$, as functions of the temperature T_L of the left (cold) reservoir (given in units of ω_c). The temperature of the right reservoir is kept fixed $T_R = 0.04\omega_c$ and $\Omega_0 = 1 \times 10^{-5}\omega_c$. The central system contains $N = 80$ atoms. The barrier has a height $k_1 = 1.5k_0$, $\sigma = a$, and moves from left to right with a speed $v = aN\Omega_0/(2\pi)$. The arrows on the horizontal axis indicate two temperature scales, T^* and $T_{\min}$, defined in the main text.

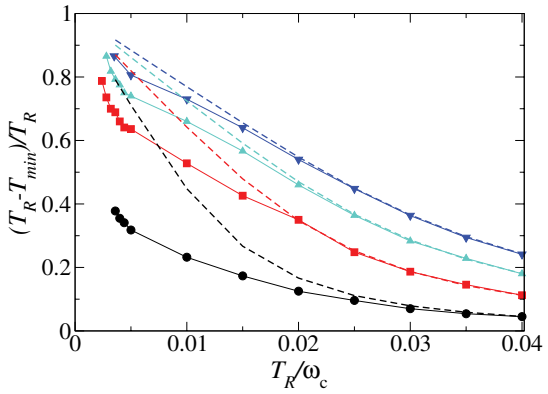

FIG. 4. (Color online) The relative temperature interval $(T_R - T_{\min})/T_R$ as a function of the right reservoir temperature T_R, where $T_{\min}$ is the minimum temperature of the left reservoir for which cooling is possible. Systems of sizes $N = 40$, 80, 120, and 160 corresponding to black circles, red squares, green downward triangles, and blue upward triangles, respectively, are considered (the solid lines are guides to the eye). For each system size, a fitting to Eq. (17) is performed (dashed lines). Other parameters are the same as in Fig. 3.

refrigerator (i.e., heat flows against the temperature gradient). It is also interesting to note that when cooling takes place ($T > T_{\min}$), the absolute values of the currents $\bar{J}^Q_{L,R}$ are approximately the same, indicating that the dissipation of energy due to the action of the external forces is very small [see Eq. (13)].

In Ref. 15, we have shown that an estimate for the temperature $T_{\min}$ is given by

$$T_{\min} = \sqrt{\sqrt{\Theta_B^4 + T_R^4} - \Theta_B^2}, \tag{17}$$

where $\Theta_B = \lambda\sqrt{5v/2\pi^3 c}$, with being c the sound velocity of the system and λ being the amplitude of a δ-function-like moving barrier [see Eq. (5) in Ref. 15]. That calculation was done in a continuous model, assuming that the moving barrier produced negligible heat. It is interesting to check if this prediction accurately describes cooling in a microscopic model and still holds when there is nonzero heat generation production by the external fields. In order to build a connection between the parameters used in these two distinct formulations, we notice that the sound velocity in the microscopic model is given by phonon velocity $c = a\sqrt{k_0/m_c}$, while the δ-funtion amplitude can be related to the substrate spring constant through $\lambda = (k_1/k_0)\mathcal{C}\,\omega_c$, where $\mathcal{C}$ is a geometrical factor related to the pulse shape.

Figure 4 shows the dependence of the lowest cooling temperature $T_{\min}$ on the hot reservoir temperature T_R for systems of several sizes and a common pumping frequency $\Omega_0 = 1 \times 10^{-5}\,\omega_c$. Notice that fixing Ω_0 requires varying the barrier speed when considering central chains of different sizes. In order to have a meaningful comparison for the different chain sizes, we present the relative difference $(T_R - T_{\min})/T_R$. The dashed lines are obtained from Eq. (17). The geometrical factor $\mathcal{C}$ is used as a fitting parameter to adjust Eq. (17) to the numerical data. The fitted values for $\mathcal{C}$ are size dependent. We find $\mathcal{C} \sim 3.6, 4.1, 4.3, 4.5$, for $N = 40, 80, 120, 160$, respectively. In all the plots, Eq. (17) provides a description of the numerical data for sufficiently high temperatures T_R. As the size of the central chain increases, the range of temperatures where Eq. (17) fits well the numerical data systematically extends to lower values of T_R. The discrepancy between Eq. (17) and the numerical data for low values T_R can be understood by noticing that for low temperatures the effect of heating due to the external fields becomes relatively large. Indeed, the effect of heating is expected to be stronger for the smaller systems, which is indeed where the discrepancy seems larger. In summary, as the size of the system increases, the behavior of the microscopic model approaches that of an infinite continuous system and the effect of heating by the external field becomes relatively insignificant. In the large-size limit, the results for the microscopic model tend to coincide with the analytical prediction of Eq. (17) and this is precisely the observed behavior in Fig. 4.

B. Cooling efficiency

The results of Sec. III A indicate that the model defined in Sec. II can be regarded as a microscopic realization of the phonon pump proposed in Ref. 15. Thus, let us consider the efficiency of the phonon refrigerator in the continuous, phonon gas model, and compare it with that of a Carnot cycle.

In Ref. 15 we showed that the heat *extracted* from the (cold) L reservoir at the end of one cycle and the heat *injected* on the (hot) R reservoir are given by

$$Q_L = -\Delta E_L^{L\to R} = \left(e_L + \frac{p_L}{\gamma\, d}\right) V_{\text{pipe}}, \tag{18a}$$

$$Q_R = +\Delta E_R^{L\to R} = \left(e_L + \frac{p_R}{\gamma\, d}\right) V_{\text{pipe}}, \tag{18b}$$

where V_{pipe} is the volume swept by the moving barrier and $e_{L,R}$ and $p_{L,R}$ are, respectively, the energy densities and the pressures in both sides of the pump. The work done in the

cycle is given by

$$W = \frac{(p_R - p_L)}{\gamma\, d}\, V_{\rm pipe}. \tag{18c}$$

The pressure and energy of a phonon gas follow the relation $p = -(\partial F/\partial V)_T = \gamma e$, where γ is the Grüneisen parameter of the lattice and d denotes the spatial dimension.[16–18]

The cooling coefficient of performance (COP) of the refrigerator is given by

$$\mathrm{COP} = \frac{Q_L}{Q_R - Q_L} = (d+1)\,\frac{p_L}{p_R - p_L}. \tag{19}$$

We can relate the pressures to the temperatures in the phonon gas in d dimensions and one finds (see Ref. 15) that $p_L/p_R = (T_L/T_R)^{d+1}$. We therefore arrive at the simple form

$$\mathrm{COP} = (d+1)\,\frac{(T_L/T_R)^{d+1}}{1-(T_L/T_R)^{d+1}}. \tag{20}$$

This cooling coefficient of performance is to be compared to that of a Carnot cycle, $\mathrm{COP}_{\rm Carnot} = \frac{(T_L/T_R)}{1-(T_L/T_R)}$. It is useful to express the ratio of these two coefficients of performance as

$$\begin{aligned}\frac{\mathrm{COP}}{\mathrm{COP}_{\rm Carnot}} &= \frac{(d+1)\,(T_L/T_R)^d}{1+(T_L/T_R)+\cdots+(T_L/T_R)^d}\\ &\leqslant 1, \quad \text{for} \quad 0 \leqslant T_L/T_R \leqslant 1.\end{aligned} \tag{21}$$

It is thus clear that the refrigerator is generically less efficient than the Carnot one. When T_L is close to T_R, the efficiency of the phonon refrigerator approaches the Carnot limit, but when $T_L \ll T_R$, the efficiency is rather low compared to that of a Carnot cycle. When $T_L/T_R = 1/2$, $\mathrm{COP}/\mathrm{COP}_{\rm Carnot} = 2/3$ for one-dimensional pipes, and $\mathrm{COP}/\mathrm{COP}_{\rm Carnot} = 4/15$ for three-dimensional systems.

IV. METHODOLOGY: GREEN FUNCTIONS AND DYSON EQUATIONS

In order to develop an analytical framework where the nonequilibrium heat currents in the microscopy phononic model can be evaluated, we follow a procedure analogous to that introduced in Ref. 19 for fermionic systems. We begin by defining the following lesser and greater Green's functions,

$$D^<_{l,l'}(t,t') = i\,\langle x_{l'}(t')x_l(t)\rangle \tag{22}$$

and

$$D^>_{l,l'}(t,t') = i\,\langle x_l(t)x_{l'}(t')\rangle, \tag{23}$$

as well as the retarded one,

$$\begin{aligned}D^R_{l,l'}(t,t') &= -i\,\Theta(t-t')\langle[x_l(t),x_{l'}(t')]\rangle\\ &= \Theta(t-t')[D^<_{l,l'}(t,t') - D^>_{l,l'}(t,t')].\end{aligned} \tag{24}$$

For coordinates along the central chain (not including the contacts), the Dyson equations for the retarded functions are

$$\begin{aligned}&-\left[\partial^2_{t'} + \frac{2k_0 + k'_l(t)}{m_c}\right] D^R_{l,l'}(t,t') + \frac{k_0}{m_c} D^R_{l,l'+1}(t,t')\\ &+ \frac{k_0}{m_c} D^R_{l,l'-1}(t,t') = \frac{1}{m_c}\delta_{l,l'}\delta(t-t').\end{aligned} \tag{25}$$

By writing the Dyson equation for D^R along the contacts, it is possible to integrate out the degrees of freedom of the reservoirs. The result is

$$\begin{aligned}&-\partial^2_{t'}\hat{D}^R(t,t') - \hat{D}^R(t,t')\hat{M}(t') - \int dt_1\,\hat{\Sigma}^R(t,t_1)\hat{D}^R(t_1,t')\\ &= \frac{1}{m_c}\delta_{l,l'}\delta(t-t'),\end{aligned} \tag{26}$$

where $\hat{M}(t) = \hat{M}^{(0)} + \hat{M}^{(1)}(t)$, with

$$M^{(0)}_{l,l'} = \begin{cases} \frac{k_0}{m_c}(2\delta_{l,l'} - \delta_{l',l\pm1}), & 1 < l < N,\\ \left(\frac{k_0}{m_c} + \frac{k_L}{m_L}\right)\delta_{l,l'} - \frac{k_0}{m_c}\delta_{l',l+1}, & l = 1,\\ \left(\frac{k_0}{m_c} + \frac{k_R}{m_R}\right)\delta_{l,l'} - \frac{k_0}{m_c}\delta_{l',l-1}, & l = N,\end{cases} \tag{27}$$

$$M^{(1)}_{l,l'}(t) = \frac{k'_l(t)}{m_c}\delta_{l,l'}, \tag{28}$$

$$\begin{aligned}\Sigma^R_{l,l'}(t,t') = \sum_{\alpha=L,R}\delta_{l',l}\,\delta_{l,l\alpha}\int_{-\infty}^{\infty}\frac{d\omega}{2\pi}e^{-i\omega(t-t')}\\ \times\int_{-\infty}^{\infty}\frac{d\omega'}{2\pi}\,\frac{\Gamma_\alpha(\omega')}{\omega-\omega'+i\eta},\end{aligned} \tag{29}$$

and

$$\begin{aligned}\Gamma_\alpha(\omega) &= \lim_{N_\alpha\to\infty}\frac{2\pi(k_\alpha/m_\alpha)^2}{N_\alpha+1}\sum_{n=0}^{N_\alpha}\sin^2\left(q^\alpha_n\right)\frac{1}{E_{\alpha,n}}\\ &\quad\times[\delta(\omega - E_{\alpha,n}) - \delta(\omega + E_{\alpha,n})]\\ &= \mathrm{sgn}(\omega)\frac{k_\alpha}{m_c}\Theta\left[1-\left(\frac{k_\alpha - m_\alpha\omega^2}{k_\alpha}\right)^2\right]\\ &\quad\times\sqrt{1-\left(\frac{k_\alpha - m_\alpha\omega^2}{k_\alpha}\right)^2}.\end{aligned} \tag{30}$$

Here, $\eta > 0$ is an infinitesimal and $E_{\alpha,n} = \sqrt{k_\alpha(1-\cos q^\alpha_n)/m_\alpha}$.

On the other hand, the Dyson equations for the lesser Green's functions read

$$D^<_{l,l'}(t,t') = \sum_\alpha\int dt_1\int dt_2\, D^R_{l,l_\alpha}(t,t_1)\,\Sigma^<_\alpha(t_1-t_2)D^A_{l_\alpha,l'}(t_2,t'), \tag{31}$$

and

$$\begin{aligned}D^<_{l,q^\alpha_n}(t,t') = -\frac{k_\alpha}{m_\alpha}\int dt_1\big[D^R_{l,l_\alpha}(t,t_1)\,d^<_{q^\alpha_n}(t_1-t')\\ + D^<_{l,l_\alpha}(t,t_1)\,d^A_{q^\alpha_n}(t_1-t')\big],\end{aligned} \tag{32}$$

where Eq. (31) corresponds to coordinates along the central chain while Eq. (32) corresponds to one coordinate along the chain and the other on the reservoir. Here we have introduced

$$\Sigma^<_\alpha(\omega) = i n_\alpha(\omega)\Gamma_\alpha(\omega), \tag{33}$$

$$d^A_{q^\alpha_n}(\omega) = \frac{1}{2E_{\alpha,n}}\left[\frac{1}{\omega - i\eta - E_{\alpha,n}} - \frac{1}{\omega - i\eta + E_{\alpha,n}}\right], \tag{34}$$

and

$$d^{<}_{q^\alpha}(\omega) = \frac{i\pi n_\alpha(\omega)}{2E_{\alpha,n}}[\delta(\omega - E_{\alpha,n}) - \delta(\omega + E_{\alpha,n})], \quad (35)$$

with $n_\alpha(\omega) = 1/(e^{\omega/T_\alpha} - 1)$ being the Bose-Einstein distribution, which depends on the temperature T_α of the reservoir α.

The strategy now is to solve Eq. (26) to evaluate the retarded function and then use the result in Eqs. (31) and (32) to calculate the lesser functions.

A. Exact solution of the Dyson equation

The exact functions $\hat{D}^R$ are obtained by solving the linear set of equations represented by Eq. (26). It is also convenient to use the representation

$$\hat{D}^R(t,t') = \sum_{k=-\infty}^{+\infty} e^{-ik\Omega_0 t} \int_{-\infty}^{+\infty} \frac{d\omega}{2\pi} e^{-i\omega(t-t')} \hat{\mathcal{D}}(k,\omega). \quad (36)$$

We get

$$\hat{D}^R(t,\omega) = \hat{D}^{(0)}(\omega) + \sum_{k\neq 0,-\infty}^{\infty} e^{-ik\Omega_0 t}\, \hat{D}^R(t,\omega + k\Omega_0) \times \hat{M}^{(1)}_k \hat{D}^{(0)}(\omega), \quad (37)$$

where we are considering the Fourier representation of the time-dependent part of the Hamiltonian, $\hat{M}^{(1)}(t) = \sum_k \hat{M}^{(1)}_k e^{-ik\Omega_0 t}$, while

$$\hat{D}^{(0)}(\omega) = [\omega^2 \hat{1} - \hat{M}^{(0)} - \hat{\Sigma}^R(\omega)]^{-1} \quad (38)$$

is the retarded Green's function corresponding to the central chain of harmonic oscillators connected to the reservoirs but free from the time-dependent modulation of the spring constants. In our case, the frequency of the ac modulation is $\Omega_0 = 2\pi/\tau = 2\pi Na/v$. The exact solution for this set of coupled linear equations can be obtained by following the procedure introduced in Ref. 19 for fermionic systems driven by ac potentials. An alternative approach, appropriate for the case of a low-frequency Ω_0 considered in the present work, is discussed in Sec. IV C.

B. dc heat currents

We now turn to the evaluation of the dc component of the heat current flowing from a given reservoir. To this end, we first express the heat current in terms of Green's functions. From Eq. (11), the dc component of the heat flow from the reservoir α can be expressed as follows:

$$\overline{J}^Q_\alpha = \mathrm{Re}\left\{ \frac{1}{\tau} \int_0^{\tau_0} dt \lim_{t'\to t} \sum_n k_{n,\alpha} \frac{-i\,\partial D^{<}_{l_\alpha,k_{n,\alpha}}(t,t')}{\partial t'} \right\}. \quad (39)$$

Using Eq. (32) and the representation shown in Eq. (36), we get

$$\overline{J}^Q_\alpha = \int \frac{d\omega}{2\pi}\omega \Big\{ 2\mathrm{Im}\big[\mathcal{D}_{l_\alpha,l_\alpha}(0,\omega)\big]\Gamma_\alpha(\omega) n_\alpha(\omega) + \sum_\beta \sum_k \big|\mathcal{D}_{l_\alpha,l_\beta}(k,\omega)\big|^2 \Gamma_\beta(\omega)\Gamma_\alpha(\omega + k\Omega_0) n_\beta(\omega) \Big\}. \quad (40)$$

The first term can be recast using Eq. (A3), leading to the following equation for the dc heat current:

$$\overline{J}^Q_\alpha = \sum_{\beta=R,L} \sum_{k=-\infty}^{+\infty} \int_{-\infty}^{+\infty} \frac{d\omega}{2\pi}(\omega + k\Omega_0)[n_\beta(\omega) - n_\alpha(\omega + k\Omega_0)]\Gamma_\alpha(\omega + k\Omega_0)\Gamma_\beta(\omega)\big|\mathcal{D}_{l_\alpha,l_\beta}(k,\omega)\big|^2. \quad (41)$$

This equation indicates that a net heat current may exist even in the absence of a temperature difference between the two reservoirs. Such a flow contains in general an incoming component which accounts for the work done by the ac fields and which is dissipated into the reservoirs. As we discuss earlier, under certain conditions, a net current between the reservoirs can be established; this current can go against a temperature gradient, therefore allowing for cooling.

In the case of a temperature difference ΔT between the reservoirs, $T_R = T_L + \Delta T$, and in stationary conditions (i.e., in the absence of ac fields), Eq. (41) reduces to Eq. (16), where $J^{(0)}_L = -J^{(0)}_R = J^{(0)}$, being the thermal transmission function, and

$$\mathcal{T}(\omega) = \Gamma_\alpha(\omega)\Gamma_\beta(\omega)\big|D^{(0)}_{l_\alpha,l_\beta}(\omega)\big|^2. \quad (42)$$

C. Low driving frequency solution of Dyson equation

Let us consider the Dyson equation in Eq. (37) in the limit of low driving frequency Ω_0.

1. First order

A solution exact up to $O(\Omega_0)$ can be obtained by expanding Eq. (37) as follows:

$$\hat{D}(t,\omega) \sim \hat{D}^{(0)}(\omega) + \hat{D}(t,\omega)\hat{M}^{(1)}(t)\hat{D}^{(0)}(\omega) + i\,\partial_\omega \hat{D}(t,\omega)\frac{d\hat{M}^{(1)}(t)}{dt}\hat{D}^{(0)}(\omega). \quad (43)$$

We define the frozen Green's function

$$\hat{D}_f(t,\omega) = [\hat{D}^{(0)}(\omega)^{-1} - \hat{M}^{(1)}(t)]^{-1}, \quad (44)$$

in terms of which the exact solution of the Dyson equation at $O(\Omega_0)$ reads

$$\hat{D}^{(1)}(t,\omega) = \hat{D}_f(t,\omega) + i\,\partial_\omega \hat{D}_f(t,\omega)\frac{d\hat{M}^{(1)}(t)}{dt}\hat{D}^{(0)}(\omega). \quad (45)$$

2. Second order

To obtain the solution exact up to $O(\Omega_0^2)$, we consider the following expansion of Eq. (37):

$$\hat{D}(t,\omega) \sim \hat{D}^{(0)}(\omega) + \hat{D}(t,\omega)\hat{M}^{(1)}(t)\hat{D}^{(0)}(\omega) + i\,\partial_\omega \hat{D}(t,\omega)\frac{d\hat{M}^{(1)}(t)}{dt}\hat{D}^{(0)}(\omega) - \frac{1}{2}\partial^2_\omega \hat{D}(t,\omega)\frac{d^2\hat{M}^{(1)}(t)}{dt^2}\hat{D}^{(0)}(\omega). \quad (46)$$

The solution exact up to $O(\Omega_0^2)$ is

$$\hat{D}^{(2)}(t,\omega) = \hat{D}_f(\omega) + i\partial_\omega \hat{D}^{(1)}(t,\omega)\frac{d\hat{M}^{(1)}(t)}{dt}\hat{D}_f(\omega) - \frac{1}{2}\partial_\omega^2 \hat{D}_f(t,\omega)\frac{d^2\hat{M}^{(1)}(t)}{dt^2}\hat{D}_f(\omega). \quad (47)$$

One can obtain this Green's function numerically by first discretizing the time in the interval $0 \leqslant t \leqslant \tau$, then solving Eq. (47) for each one time, and finally evaluating the Fourier transform to obtain the Floquet representation, with which the dc component of the heat current can be calculated from Eq. (41).

D. Low driving frequency expansion of the dc heat current

Let us now use the low-frequency expansion in the expression of dc heat current flowing into the reservoir α given by Eq. (41). We first expand $n_\alpha(\omega + k\Omega_0)$ and $\Gamma_\alpha(\omega)$ in powers of Ω_0. By keeping terms up to $O(\Omega_0^2)$, we can identify the following decomposition in the net current flowing into the reservoir:

$$\overline{J}_\alpha^Q = \overline{J}_\alpha^{th} + \overline{J}_\alpha^{p} + \overline{J}_\alpha^{th-p} + \overline{J}_\alpha^{d}, \quad (48)$$

where "thermal" component $\overline{J}_\alpha^{th}$ is due to the gradient of temperature and flows from the hot to the cold reservoir, the "pumped" component $\overline{J}_\alpha^{p}$ is purely induced by the driving and accounts for the cooling mechanism, the "mixed" component $\overline{J}_\alpha^{th-p}$ results from an interference process of the temperature gradient and the cooling mechanism, while the "dissipative" term $\overline{J}_\alpha^{d}$ accounts for the dissipation of energy into the reservoir due to the action of the ac fields.

The explicit expression for the thermal component is

$$\overline{J}_\alpha^{th} = \int \frac{d\omega}{2\pi}[n_\beta(\omega) - n_\alpha(\omega)]\omega\mathcal{T}_f(\omega), \qquad \mathcal{T}_f(\omega) = \Gamma_\alpha(\omega)\left|\mathcal{D}_{f,l_\alpha,l_\beta}(0,\omega)\right|^2\Gamma_\beta(\omega), \quad (49)$$

with $\beta \neq \alpha$, while $\mathcal{D}_{f,l_\alpha,l_\beta}(0,\omega)$ is the dc component matrix element of the frozen Green's function (44). Notice that $\overline{J}_L^{th} = -\overline{J}_R^{th}$. Also, recalling that the left reservoir is the cold one, $\overline{J}_L^{th} > 0$, indicating that this component flows from right to left. It is also interesting to note that the frozen transmission function corresponds to the chain with the barrier. Thus, it is practically vanishing for small $|\omega|$, as shown in Fig. 2.

In order to write an expression for the pumped component, we take as a reference temperature the one corresponding to the cold reservoir, T_L, resulting in

$$\overline{J}_\alpha^{p} = \sum_{\beta=L,R}\sum_k \int \frac{d\omega}{2\pi}\omega k\Omega_0\left(-\frac{dn_L(\omega)}{d\omega}\right) \times \Gamma_\alpha(\omega)\left|\mathcal{D}_{f,l_\alpha,l_\beta}(k,\omega)\right|^2\Gamma_\beta(\omega). \quad (50)$$

In Appendix B we show that $\overline{J}_L^{p} = -\overline{J}_R^{p}$. In our case, the driving mechanism is designed to cool the left reservoir, thus $\overline{J}_L^{p} < 0$, and this current flows against the temperature gradient. This component is $\propto \Omega_0$ and we neglect eventual contributions $\propto \Omega_0^2$ or terms of higher order in Ω_0.

The mixed components read

$$\overline{J}_L^{th-p} = \sum_k \int \frac{d\omega}{2\pi}[n_R(\omega) - n_L(\omega)]\omega k\Omega_0 \times \frac{\partial\Gamma_L(\omega)}{\partial\omega}|\mathcal{D}_{f,1,N}(k,\omega)|^2\Gamma_R(\omega),$$

$$\overline{J}_R^{th-p} = \overline{J}_{R,0}^{th-p} - \overline{J}_L^{th-p},$$

$$\overline{J}_{R,0}^{th-p} = -\sum_{\beta=L,R}\sum_k \int \frac{d\omega}{2\pi}\omega k\Omega_0\frac{\partial^2 n_L(\omega)}{\partial\omega\partial T}\Delta T \times \Gamma_L(\omega)\left|\mathcal{D}_{f,1,l_\beta}(k,\omega)\right|^2\Gamma_\beta(\omega), \quad (51)$$

which are $\propto \Omega_0\Delta T$, being $\Delta T = T_R - T_L$. Approximating the integrand of the last term, $\partial^2 n_L/(\partial\omega\partial T_L) \sim \partial n_L/(T_L\partial\omega)$, which is the leading contribution in ω/T_L, we get $\overline{J}_{R,0}^{th-p} \sim \Delta T\overline{J}_R^{p}/T_L = -\Delta T\overline{J}_L^{p}/T_L$.

Finally, in $\overline{J}_\alpha^{d}$, for which we do not provide the explicit expression for sake of simplicity, we collect all the terms that are $\propto \Omega_0^2$ and satisfy $\overline{J}_\alpha^{\rm dis} > 0$, $\alpha = L,R$. Thus, this contribution describes pure dissipation of heat generated by the ac fields that flows into the reservoirs. This contribution is vanishing small for small Ω_0.

V. SUMMARY AND CONCLUSIONS

We have considered a microscopic model for the phononic refrigeration mechanism proposed in Ref. 15. The model describes a one-dimensional lattice of atoms or molecules with identical masses connected by springs and in contact with cold and hot reservoirs at its ends. Considering only longitudinal vibrational modes, a moving "barrier" is realized by applying a local harmonic time-dependent pinning potential to the masses. The cooling cycle consists of propagating the barrier along the chain, going from the cold to the hot reservoir with constant speed. When it reaches the hot reservoir, the barrier is returned to near the cold reservoir and the cycle is repeated. We have shown that such a perturbation, when static, suppresses transmission within the low-energy sector of the phononic spectrum. In this sense, our model describes a situation similar to that found in electrostrictive polymer systems discussed in Ref. 20, where an electric field is used to open a local phonon gap.

The Hamiltonian described in Eq. (2) could be realized experimentally in several ways. For instance, in the case of a chain consisting of polarizable molecules, the local pinning of intermolecular vibrations could be achieved through the application of a inhomogeneous electric field, which would be swept along the chain to produce a moving phonon barrier.

We note that the static version of the model described in Sec. II is rather standard in the study of heat transport along harmonic chains with a single mass per unit cell, including terms beyond the usual intermass coupling but within the harmonic approximation.[10] In our case, we have considered a

time-dependent version of those extensions in order to model the moving barrier.

The evaluation of heat currents requires the use of a formulation capable of handling both a temperature gradient and the time-dependent perturbation simultaneously. To that end, we employed an analytical approach based on nonequilibrium Green's functions. This treatment is similar to the one introduced to study electronic systems driven out of equilibrium by harmonic time-dependent voltages; here, it was suitably adapted to phonon propagators.[19] We have also introduced a particular strategy that allows for solving Dyson equations in the limit of weak driving frequencies and large amplitudes. The propagators can then be evaluated numerically through a time discretization and Fourier transform.

ACKNOWLEDGMENTS

This work is supported in part by ANPCyT and CONICET in Argentina, the J. S. Guggenheim Memorial Foundation (L.A.), DOE Grant No. DE-FG02-06ER46316 (C.C.), and CAPES, CNPq, FAPERJ, and INCT-Nanomateriais de Carbono in Brazil (R.B.C.).

APPENDIX A: AN IMPORTANT IDENTITY

Following the same steps of Ref. 3, we start from the very definition of the retarded function in Eq. (24). Then, using the representation of Eq. (36), we obtain

$$\int_{-\infty}^{t} dt' e^{i(\omega+i\eta)(t-t')}\Theta(t-t')D^{<,>}_{l,l'}(t,t') = \sum_{k_1,k_2}\sum_{\alpha=R,L}\int_{-\infty}^{+\infty}\frac{d\omega_1}{2\pi} \times \frac{D_{l,l_\alpha}(k_1,\omega_1)\Gamma_\alpha(\omega_1)D^*_{l',l_\alpha}(k_2,\omega_1)\lambda^{<,>}_\alpha(\omega)}{\omega+i\eta-(\omega_1+k_2\Omega_0)}, \quad \text{(A1)}$$

with $\lambda^{<}_\alpha(\omega) = -n_\alpha(\omega)$ and $\lambda^{>}_\alpha(\omega) = -[1-n_\alpha(\omega)]$. Therefore,

$$\mathcal{D}_{l,l'}(k,\omega) = \sum_{k_1}\sum_{\alpha=R,L}\int_{-\infty}^{+\infty}\frac{d\omega_1}{2\pi} \times \frac{\mathcal{D}_{l,l_\alpha}(k_1,\omega_1)\Gamma_\alpha(\omega_1)\mathcal{D}^*_{l',l_\alpha}(k_2,\omega_1)}{\omega+i\eta-(\omega_1+k_2\Omega_0)}, \quad \text{(A2)}$$

which implies the following identity:

$$\mathcal{D}_{l,l'}(k,\omega) - \mathcal{D}^*_{l',l}(-k,\omega+k\Omega_0) = -i\sum_{k'},\sum_{\alpha=R,L}\mathcal{D}_{l,l_\alpha}(k+k',\omega-k'\Omega_0) \times \Gamma_\alpha(\omega-k'\Omega_0)\mathcal{D}^*_{l',l_\alpha}(k',\omega-k'\Omega_0). \quad \text{(A3)}$$

APPENDIX B: CONSERVATION OF THE PUMPED COMPONENT OF THE NET HEAT CURRENT

The goal of this appendix is to show that the pumped dc heat current [Eq. (50)] is conserved, in the sense that it satisfies

$$\sum_{\alpha=L,R}\overline{J}^p_\alpha = 0. \quad \text{(B1)}$$

To this end, we use the relation between the frozen Green's function and the frozen scattering matrix,[19]

$$S_{\alpha\beta}(k,\omega) = \delta_{\alpha,\beta}\delta_{k,0} - i\sqrt{\Gamma_\alpha(\omega)}\mathcal{D}_{f,l_\alpha,l_\beta}(k,\omega)\sqrt{\Gamma_\beta(\omega)}, \quad \text{(B2)}$$

and recast Eq. (50) as

$$\overline{J}^p_\alpha = \frac{1}{\tau}\int_0^\tau dt\int\frac{d\omega}{2\pi}\omega\left(-\frac{\partial n_L(\omega)}{\partial\omega}\right)\mathrm{Im}[\hat{S}(t,\omega)\partial_t\hat{S}^\dagger(t,\omega)], \quad \text{(B3)}$$

which has been proved to satisfy Eq. (B1) on the basis of the Birman-Krein relation, $d\ln(\det\hat{S}) = \mathrm{Tr}(\hat{S}d\hat{S}^\dagger)$ [where $\det(\hat{X})$ and $\mathrm{Tr}(\hat{X})$ are the determinant and the trace of a matrix $\hat{X}$, respectively], applied to the frozen matrix, which is unitary.[3,7]

[1]For a recent review, see A. Cho, Science **327**, 516 (2010).
[2]F. Giazotto, T. T. Heikkilä, A. Luukanen, A. M. Savin, and J. P. Pekola, Rev. Mod. Phys. **78**, 217 (2006); J. T. Muhonen, M. Meschke, and J. P. Pekola, Rep. Prog. Phys. **75**, 046501 (2012).
[3]L. Arrachea, M. Moskalets, and L. Martin-Moreno, Phys. Rev. B **75**, 245420 (2007); L. Arrachea and M. Moskalets, in *Handbook on Nanophysics*, edited by K. Sattler (Taylor and Francis, Boca Raton, 2010).
[4]M. Rey, M. Strass, S. Kohler, P. Hänggi, and F. Sols, Phys. Rev. B **76**, 085337 (2007).
[5]S. Zippilli, G. Morigi, and A. Bachtold, Phys. Rev. Lett. **102**, 096804 (2009); S. Zippilli, A. Bachtold, and G. Morigi, Phys. Rev. B **81**, 205408 (2010); E. J. McEniry, T. N. Todorov, and D. Dundas, J. Phys.: Condens. Matter **21**, 195304 (2009); M. Galperin, K. Saito, A. V. Balatsky, and A. Nitzan, Phys. Rev. B **80**, 115427 (2009); F. Pistolesi, J. Low Temp. Phys. **154**, 199 (2009); F. Santandrea, L. Y. Gorelik, R. I. Shekhter, and M. Jonson, Phys. Rev. Lett. **106**, 186803 (2011).
[6]D. J. Thouless, Phys. Rev. B **27**, 6083 (1983).
[7]P. W. Brouwer, Phys. Rev. B **58**, R10135 (1998); M. Moskalets and M. Büttiker, *ibid.* **66**, 035306 (2002); J. E. Avron, A. Elgart, G. M. Graf, and L. Sadun, Phys. Rev. Lett. **87**, 236601 (2001).
[8]P. Sharma and C. Chamon, Phys. Rev. Lett. **87**, 096401 (2001); E. R. Mucciolo, C. Chamon, and C. M. Marcus, *ibid.* **89**, 146802 (2002).
[9]E. Fermi, J. Pasta, and S. Ulam, Los Alamos Report LA-1940, 1955 (unpublished).
[10]S. Lepri, R. Livi, and A. Politi, Phys. Rev. Lett. **78**, 1896 (1997); M. Terraneo, M. Peyrard, and G. Casati, *ibid.* **88**, 094302 (2002); N. Li, B. Li, and S. Flach, *ibid.* **105**, 054102 (2010); A. Dhar, Adv. Phys. **57**, 457 (2008).
[11]M. Büttiker, Phys. Rev. Lett. **57**, 1761 (1986); T. Gramespacher and M. Büttiker, Phys. Rev. B **56**, 13026 (1997); L. Arrachea, C. Naón, and M. Salvay, *ibid.* **77**, 233105 (2008).
[12]D. Segal, J. Chem. Phys. **130**, 134510 (2009).
[13]B. K. Agarwalla, J.-S. Wang, and B. Li, Phys. Rev. E **84**, 041115 (2011).

[14]J. Ren, P. Hänggi, and B. Li, Phys. Rev. Lett. **104**, 170601 (2010).
[15]C. Chamon, E. R. Mucciolo, L. Arrachea, and R. B. Capaz, Phys. Rev. Lett. **106**, 135504 (2011).
[16]N. W. Ashcroft and N. D. Mermin, *Solid State Physics* (Saunders College, Philadelphia, 1976).
[17]R. S. Sorbello, Phys. Rev. B **6**, 4757 (1972).
[18]Y. C. Lee and W. Z. Lee, Phys. Rev. B **74**, 172303 (2006).
[19]L. Arrachea, Phys. Rev. B **72**, 125349 (2005); L. Arrachea and M. Moskalets, *ibid*. **74**, 245322 (2006); L. Arrachea, *ibid*. **75**, 035319 (2007).
[20]M. G. Menezes, A. Saraiva-Souza, J. Del Nero, and R. B. Capaz, Phys. Rev. B **81**, 012302 (2010).